Jefferson Lab
E94010 Technical Note 32
July 2000

Analysis of the Hall A HRS Čerenkov Detectors for E94010

K. Slifer
Temple University, Philadelphia, PA 19122
E-mail
kslifer@thunder.temple.edu

Abstract

We discuss the Hall A HRS Čerenkov detectors as used in experiment E94010. A calibration of the Čerenkov is performed. Detection and cut efficiencies are evaluated. The effect of the particle I.D. cut on pion contamination is presented.

Contents

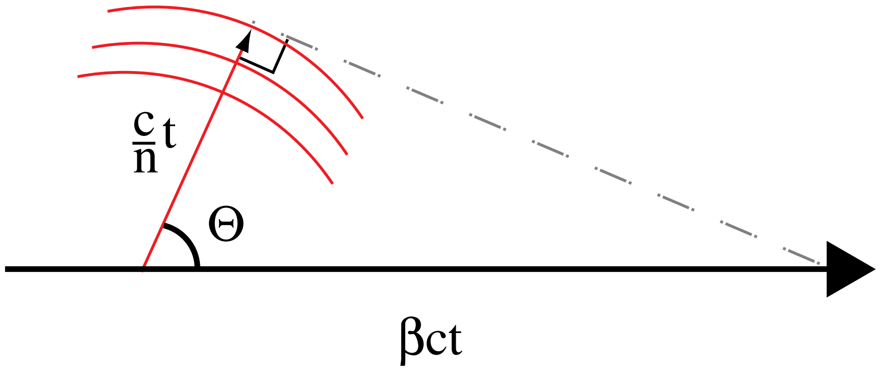

Figure 1: **Čerenkov Radiation**

1 Introduction

1.1 The Čerenkov Effect

The velocity of light is reduced when travelling through a transparent medium such as a gas, so that a high energy particle with velocity βc may exceed the velocity of light $\frac{c}{n}$ within the medium. The particle's velocity is still limited to the speed of light in vacuum, c. When this happens, an "electromagnetic shockwave" [1] occurs which is analogous to a sonic boom created by a supersonic aircraft. The threshold for production of Čerenkov radiation is:

$$\beta c \geq \frac{c}{n} \tag{1}$$

or

$$\beta \geq \frac{1}{n} \tag{2}$$

The wave is emitted in a conical pattern as shown in Fig. 1, with half angle θ given by:

$$\cos\theta = \frac{\frac{c}{n}t}{\beta ct} \tag{3}$$

or

$$\cos\theta = \frac{1}{\beta n} \tag{4}$$

The existence of a threshold which depends on velocity makes the detection of Čerenkov light a very effective method to discriminate between particle species of differing mass.

1.2 The Hall A Čerenkov Detectors

The Hall A Electron Arm and Hadron Arm High Resolution Spectrometers (HRS) both possess threshold gas Čerenkov detectors for use in particle identification. The Čerenkov tanks utilize atmospheric pressure CO_2 with an index of refraction of 1.00041 [2]. This results in a half-cone angle θ of roughly 1.6 degrees. Using equation (2) and the fact that

$$\gamma = \sqrt{\frac{1}{1-(\beta c)^2}} \tag{5}$$

and

$$E = \gamma mc^2 = \sqrt{m^2c^4 + p^2c^2} \tag{6}$$

we can easily determine the threshold energy for production of Čerenkov radiation for electrons and for pions. We find that:

$$p_{min,e} = 17.85MeV/c \tag{7}$$

while

$$p_{min,\pi} = 4.87GeV/c \tag{8}$$

The range of spectrometer momenta covered in experiment E94010 is roughly 300 MeV/c to 3.6 GeV/c. For all these settings, incident electrons will radiate Čerenkov light, while pions will not. This provides the primary method of removing pion contamination from the data.

1.2.1 Čerenkov detector details

The two detectors have identical cross-sections but differing lengths. The electron arm detector is 1.5 m long while the hadron detector is only 1.0 m in length. The detectors house 10 rectangular profile, spherical mirrors. Each mirror is positioned to reflect collected light to a dedicated photo-multiplier tube (Burle 8854) [2]. The mirrors sit in two columns of 5 at the rear of the tanks, and are made of light-weight ($\sim 5.5 \times 10^{-3}$ radiation lengths) materials to minimize attenuation of the incident electrons.

2 Calibration

Ultimately, the 10 photo-multiplier tube outputs are summed, and a cut on the final ADC distribution is used to discriminate pions from electrons. Before this can be done, the offsets and gains of the tubes must be adjusted by editing the relevent lines in the detector database. The Čerenkov coefficients are located immediately following the VDC information. Layouts can vary slightly, but for an E94010 compatible database the electron arm values should be on or near lines 805 & 806, while the hadron values should be on or near lines 1621 & 1622. For more information regarding the layout of the database see [4] and [6]. The first 10 values

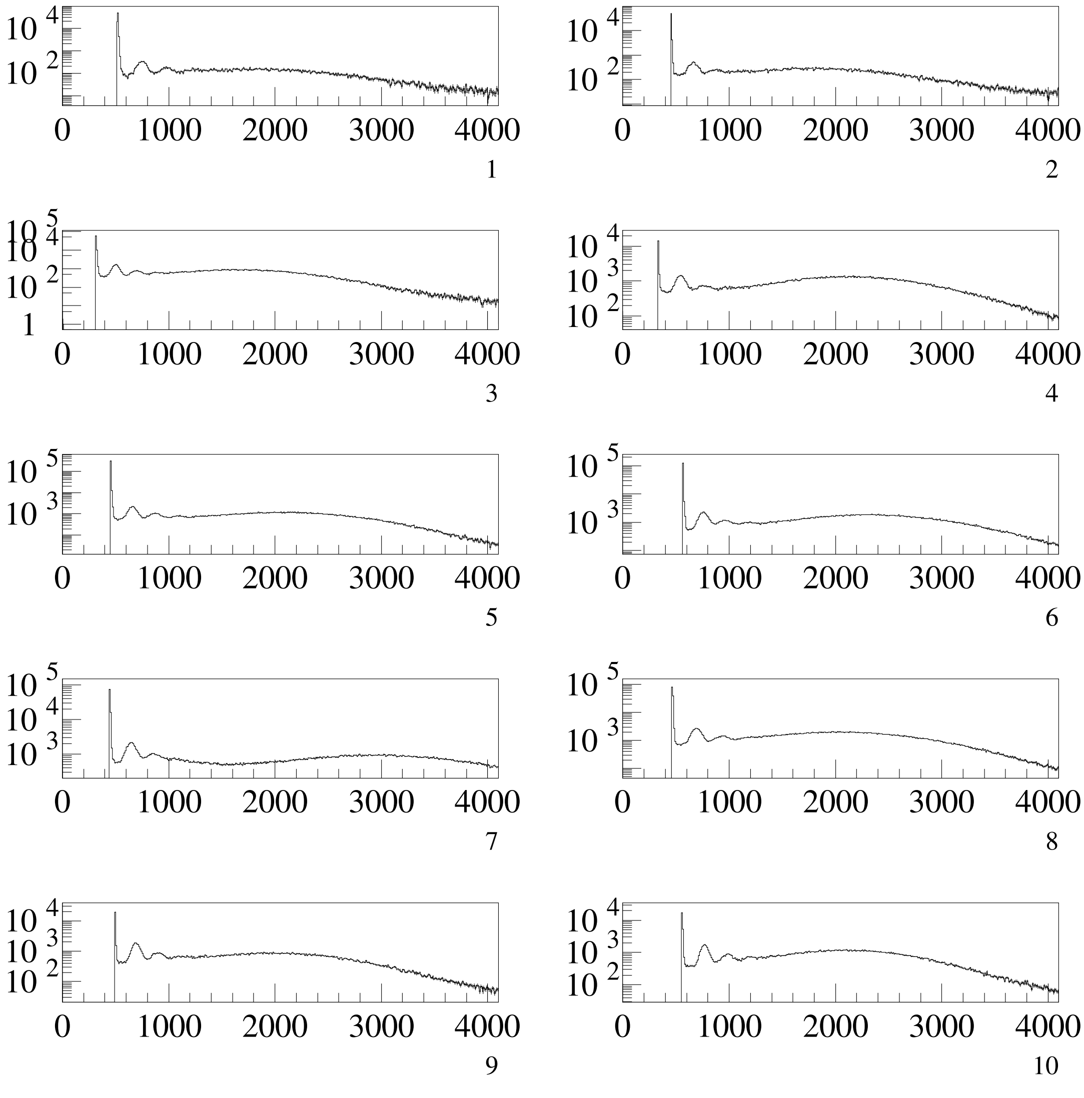

Figure 2: **Raw Čerenkov ADC.** We show here Espace variable spec.e.gas.adc

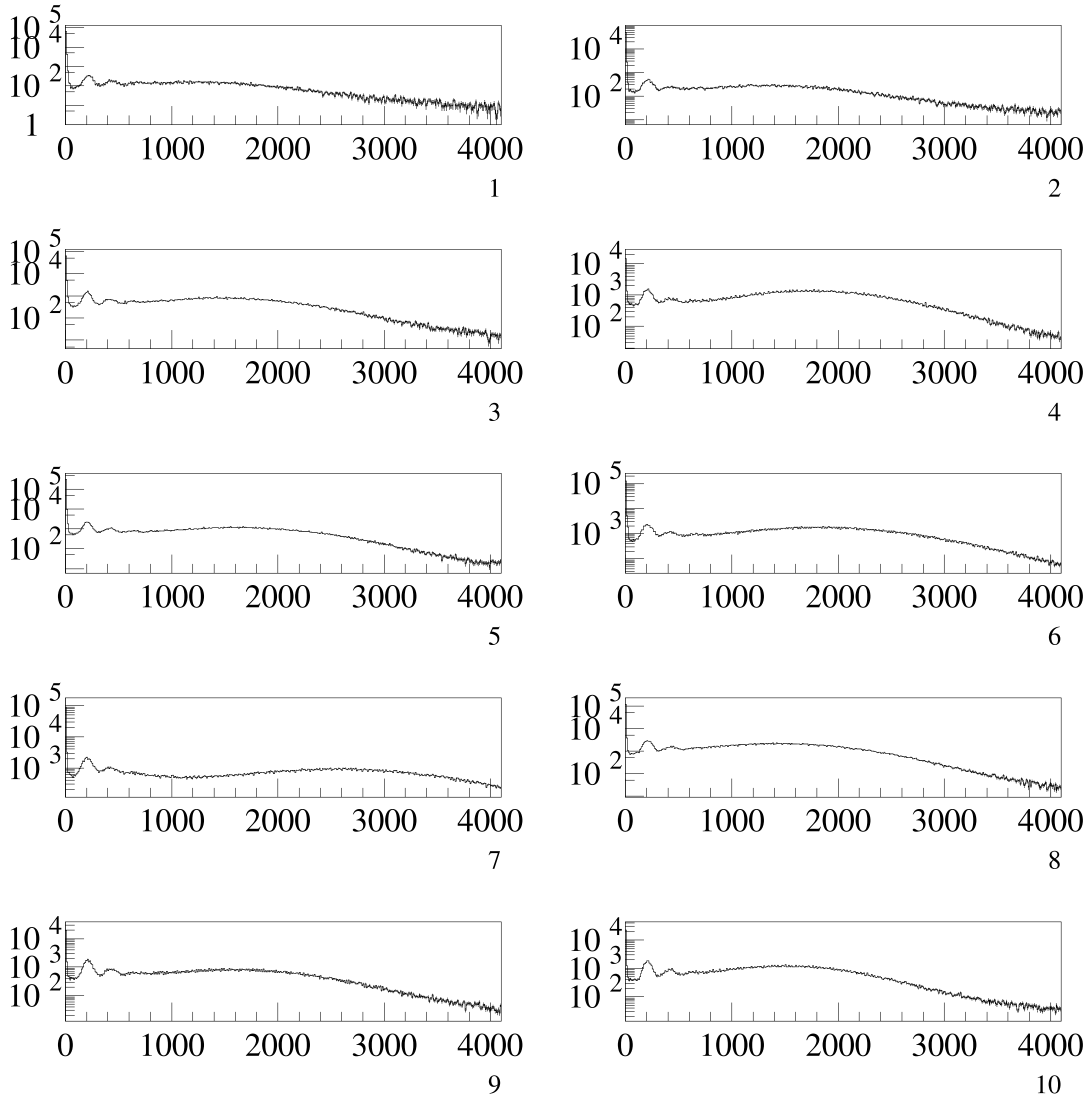

Figure 3: **Calibrated Čerenkov ADC.** We show here Espace variable spec.e.gas.adc_c

represent the channel location of the pedestal while the second 10 represent the software gain to be applied to each ADC output.

Pedestal location can be accomplished using Espace [6] by decreasing the bin size to 1 or 5 channels per bin and observing the raw Čerenkov ADC as follows:

```
set/spectrum/bins/x1 1
set/spectrum/window/x1 0 4000
do i = 1,10
spectra/save spec_e.gas.adc[[i];[i]]
enddo
```

Once the pedestals have been entered into the database, a second pass is made to adjust the software gain. Now we look at the corrected Čerenkov ADC spectra:

```
do i = 1,10
spectra/save spec_e.gas.adc_c[[i];[i]]
enddo
```

The software gain is correctly set by lining up the highly visible single photo-electron peaks. Figs. 2 and 3 show the ADC outputs for the 10 electron arm mirrors before and after the gain and pedestal adjustment have been made. Notice that the maximum of the overall distributions are *not* aligned. We compensate for the high-voltage gains of the dynode chain when we adjust the software gain, but there are several other factors that affect the photo-tube output. The broad peak is related to the average number of photo-electrons produced by the cathode, and this is affected by the quantumn efficiency of the cathode and by the intensity of illumination. We know that the mirrors are not illuminated identically because of their different positions in the transverse plane. Each mirror samples a unique value of scattering angle and of particle momenta. Also, the differences in distribution max reflects the differing efficiencies of each photo-cathode to emit an electron for a given amount of light. For example, we see that photo-cathode #7 is able to emit more electrons, on average, for a given amount of light than its neighbors. It is not surprising that the photo-tubes differ in this manner, because of the uncertainty involved in the coating of the photo-tube entrance windows with a wavelength shifter to enhance efficiency [3]. Ultimately a cut is made just below the single photo-electron peak and it is necessary for the single photo-electron peaks to be aligned for this to cut to be applied effectively.

Final results for the E94010 calibration can be found in database ~/slifer/ceren/db_feb02 on CUE machines at JLAB.

2.1 Stability

Calibration would need to be repeated for each momentum setting if it was found that the ADC output of the photo-tubes changed in any substantial way over time, or if a momentum dependence was observed. Fig. 4 shows a plot of the single photo-electron peak (averaged

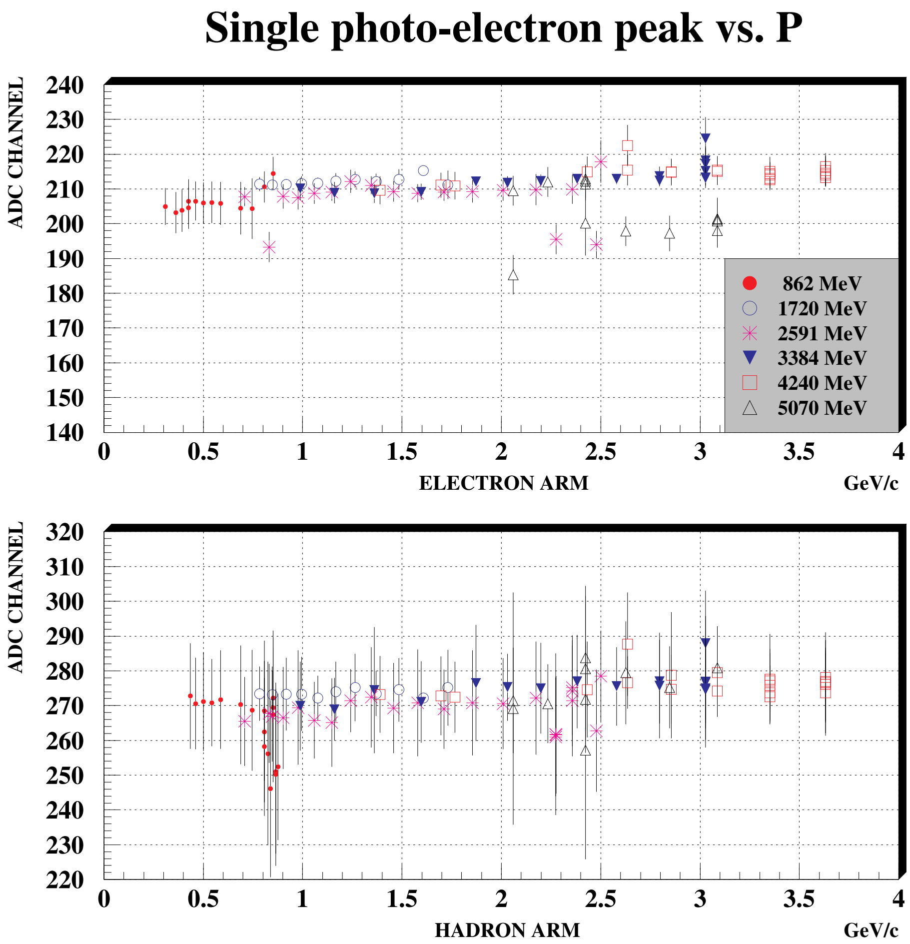

Figure 4: **Stability of Cerenkov Detectors.** Data points represent the single photo-electon peak averaged over 10 mirrors. The error bars measure the spread of the ten values. The outliers in the Electron Arm below channel 200 represent data that was taken with a lowered scintillator trigger threshold during the period Dec. 11-21, 1998.

over ten mirrors) as a function of spectrometer central momentum for all six incident energies. The vertical axis represents ADC channel location of the single photo-electron peak. It can be seen that the output is quite stable except for a few settings in the 2.5 GeV and 5.1 GeV data. This data was taken late in the experiment (Dec. 11-21, 1998) when the scintillator trigger thresholds were lowered (See discussion in Reference [5]). This data should be used with care as the lower scintillator threshold significantly affects the detected yield at these settings.

3 Detection Efficiency

For a Poisson distribution, such as the Čerenkov ADC spectrum, with a mean value μ, $e^{-\mu}$ is the probability of emitting zero photoelectrons. The detection efficiency can therefore be expressed as:

$$\epsilon = 1 - e^{-\mu} \tag{9}$$

The average number of photoelectrons produced per meter, μ, has been evaluated previously to be approximately nine [2], so we expect an efficiency of roughly 99.99%.

The detection efficiency is measured as the fraction of good electron events that trigger the Čerenkov. In the electron arm, this ratio is measured by putting a tight 2-dimensional cut on the total shower to select good electrons. (See Fig. 5.) Then we simply count how many of these electrons are also detected by the Čerenkov detector. For the Hadron arm we proceed in the same fashion. However, there is only a single thin layer of lead-glass in the Hadron arm calorimeter. As such, only a one-dimensional cut is possible (See Fig. 6).

Overall results for both detectors can be seen in Fig. 7. Note that the detection efficiency appears to be a strong function of ν=E-E', so that runs with identical momenta but with differing incident energy can have greatly different efficiency. We argue that this is an artefact of the method used to determine efficiency. At large ν there is greater phase space for production of pions. Pions do not trigger the Čerenkov but they *are* detected in the calorimeter. As such they appear as lost events in an efficiency calculation. The tight cuts on the shower detector are intended to remove pions from the data, but there is invariably some pion contamination. The fact that only a 1-D cut is available for the Hadron arm results in a higher percentage of pions in our "good" data set and an apparently degraded efficiency at large ν. This effect can be seen clearly in Fig. 6, where the hashed distribution represents any events in the Hadron shower that have not triggered the Čerenkov. These events are a continuous tail of the pion peak seen at the left of the graph and therefore do not represent a true detection inefficiency. To check the above assumptions, we selected several runs with overlapping central momentum E', but with differing incident energy E. No difference in the measured number of photoelectrons produced by the mirrors was observed, nor was there any other change in the behaviour of the Čerenkov. The only difference observed was a large pion contamination for the runs with degraded efficiency.

We conclude, by observing the results were pion production is low, that the detection efficiency of the Electron arm Čerenkov is better than 99.9%, while the Hadron arm performs to better than 99.5%. The slight overall difference is expected as a result of the extended length of the Electron arm Čerenkov tank.

4 Cut Efficiency

A cut below the single photo-electron peak to channel 16000 is applied to both Čerenkov detectors to remove pions and low energy events. This will invariably remove good events from the data as well. Estimates of the lost events can be obtained by fitting the Čerenkov distribution and counting the events excluded by the cuts. In Figs. 8 and 9, we see the resulting efficiency for three different choices of cuts. It is found that a cut from channel 150-16000 results in less than 1% loss for both detectors for virtually all kinematic settings. From Fig. 4 we know that the cut is being applied below the single photo-electron peak for all runs.

The final particle I.D. cut involves a cut on the Čerenkov and the Shower detector [5]. The net result of these cuts on the pion contamination is shown in Fig. 10

5 Conclusion

The Hall A Čerenkov detectors have been calibrated and shown to be stable throughout the experiment, although care must be exercised when using data from Dec. 11-21, 1998 because of the altered yield. The detection efficiency is found to be extremely good. Cuts have been chosen and the resulting cut efficiency evaluated. A database named "db_feb02" that includes the corrected offsets and gains can be found in the directory ~/slifer/ceren on CUE machines at JLAB.

6 Acknowledgments

I would like to thank Zein-Eddine Meziani and Seonho Choi for their valuable advice.

References

[1] William R. Leo,"*Techniques for Nuclear and Particle Physics Experiments.*", pg.33 (1987).

[2] M. Iodice,et al."*The CO_2 Gas Cherenkov Detectors for the Jefferson Lab Hall-A Spectrometers*", Elsevier Preprint (January 1998)

[3] Sue Duncan, et al., "*Effect of P-Terphenl Coating to the Quantum Efficiency of Burle 8854 Photomultiplier Tubes*", Jefferson Lab Technical Note JLAB-TN-98-006.

[4] Luminita Todor,"*Hall A Detector Database Calibration* ", VCS Technical Note (June 1998).

[5] K. Slifer, "*Shower Detector Calibration and Cut Optimization for E94010*", E94010 Technical Note (May 2000).

[6] "*ESPACE User's Guide* ", http://hallaweb.jlab.org/espace/index.html

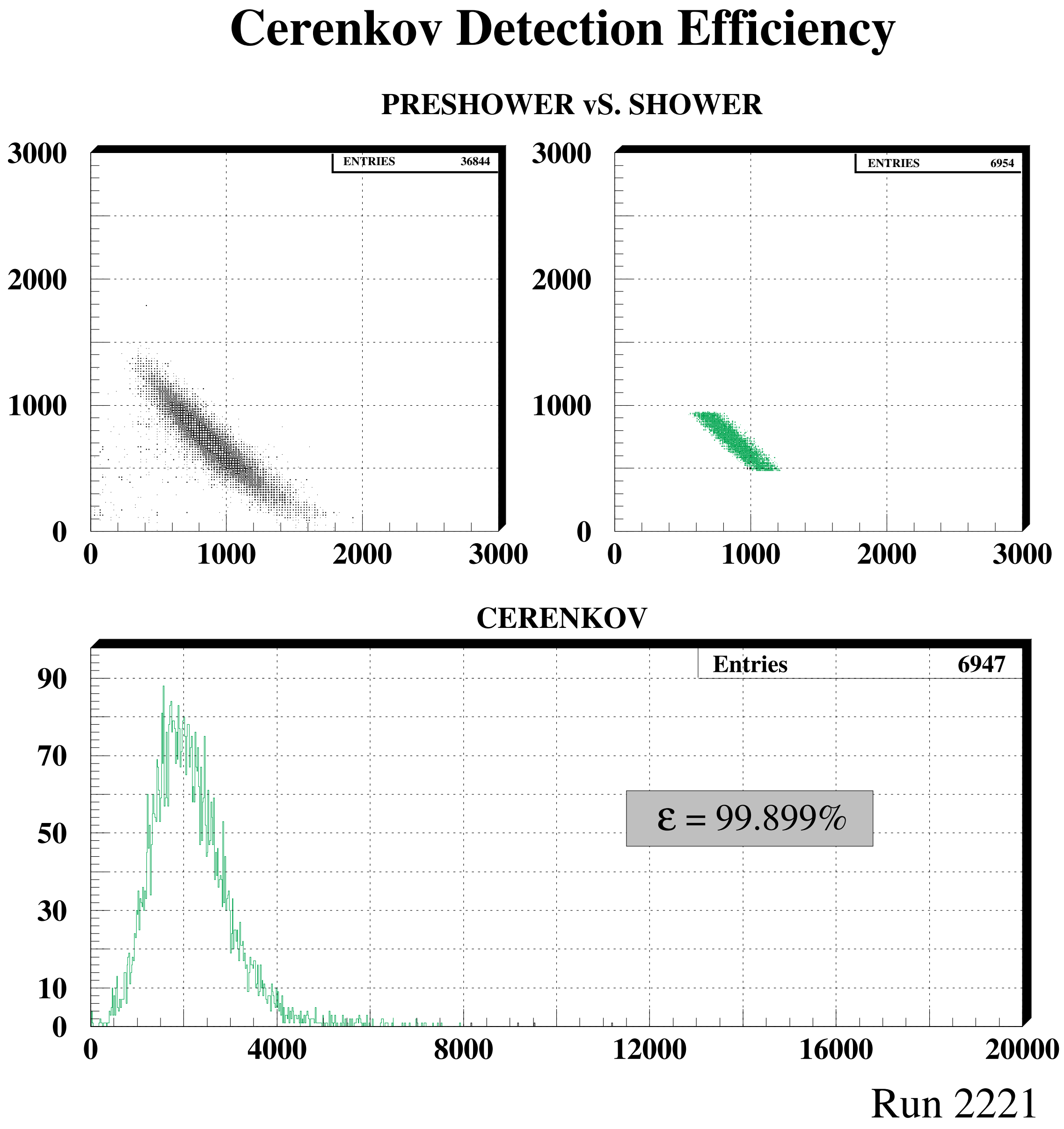

Figure 5: **Detection Efficiency of Electron arm Čerenkov Detector.** *Upper left:* Graph of calibrated preshower cluster vs. shower cluster. *Upper right:* Tight cut used to select good electrons. *Lower:* Cerenkov ADC after above 2-D cut is applied.

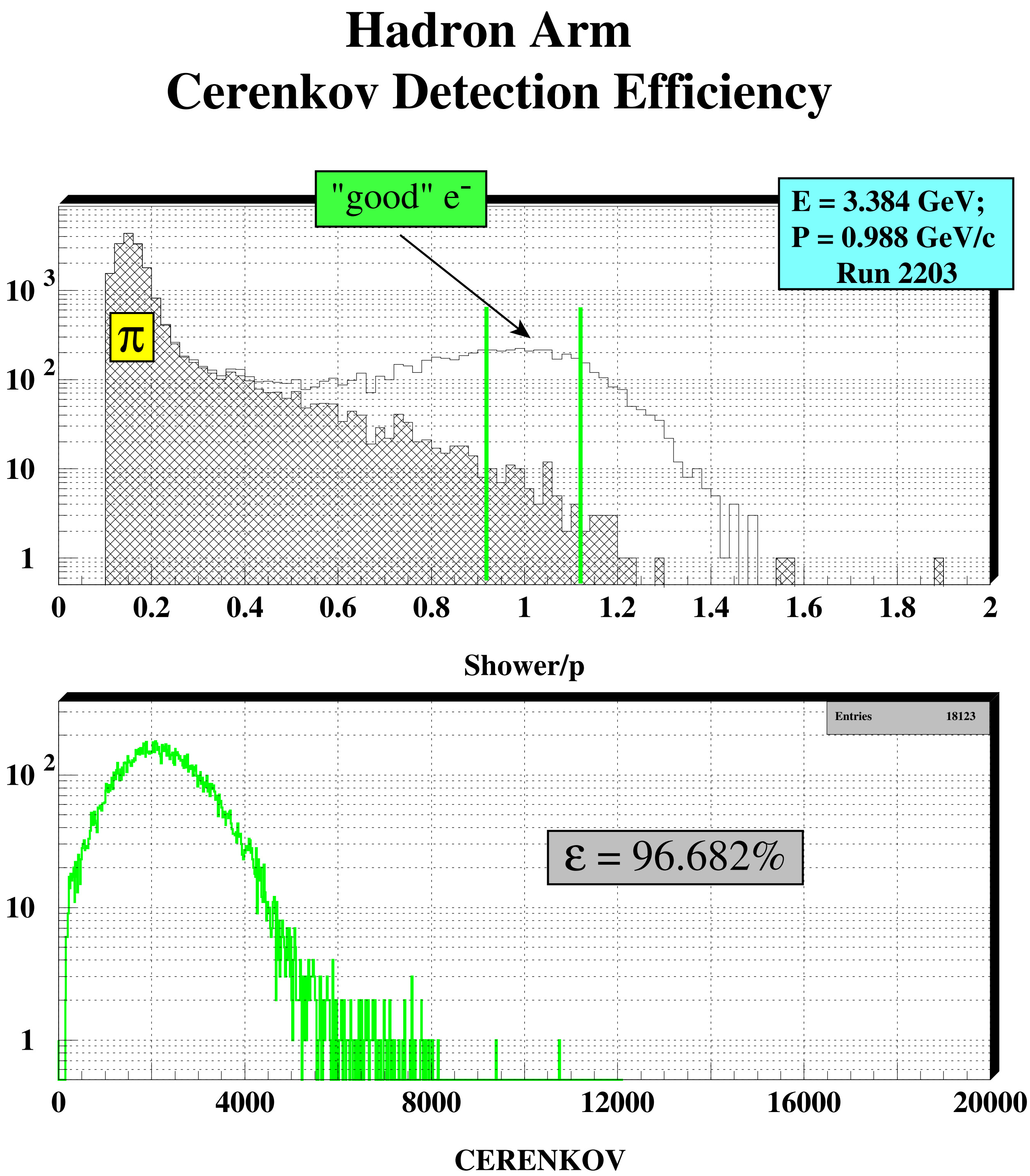

Figure 6: **Detection Efficiency of Hadron arm Čerenkov Detector.** *Upper :* Graph of calibrated shower output normalized by momentum. Good events used in the efficiency calculation are within the tight cut. The hashed distribution are any events that have not triggered the the Čerenkov. *Lower:* Hadron Arm Čerenkov after application of above mentioned tight cut.

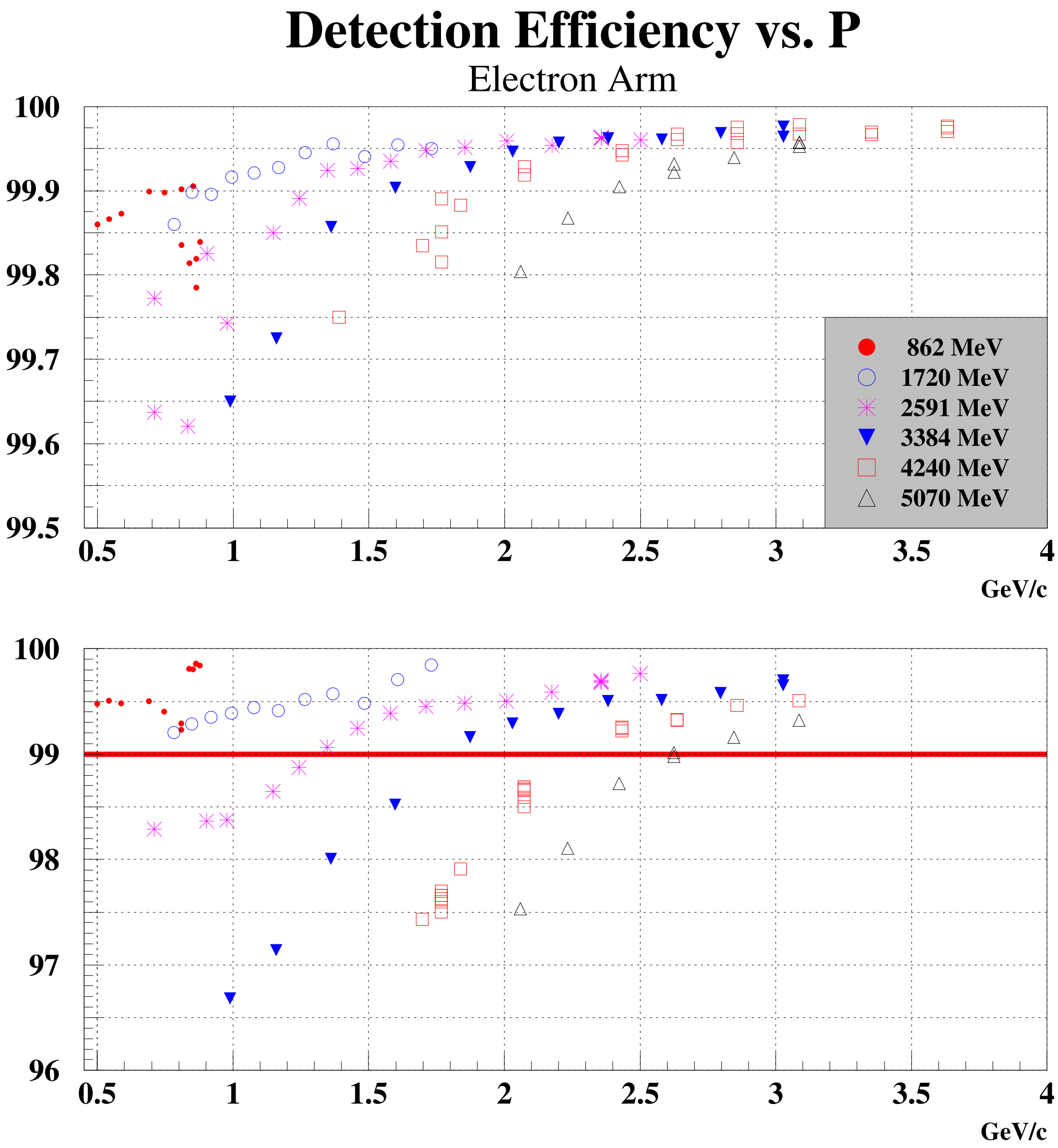

Figure 7: **Detection Efficiency as a function of momentum.** The apparent degradation of efficiency with increasing $\nu = E - E'$ is the result of pion contamination at large ν.

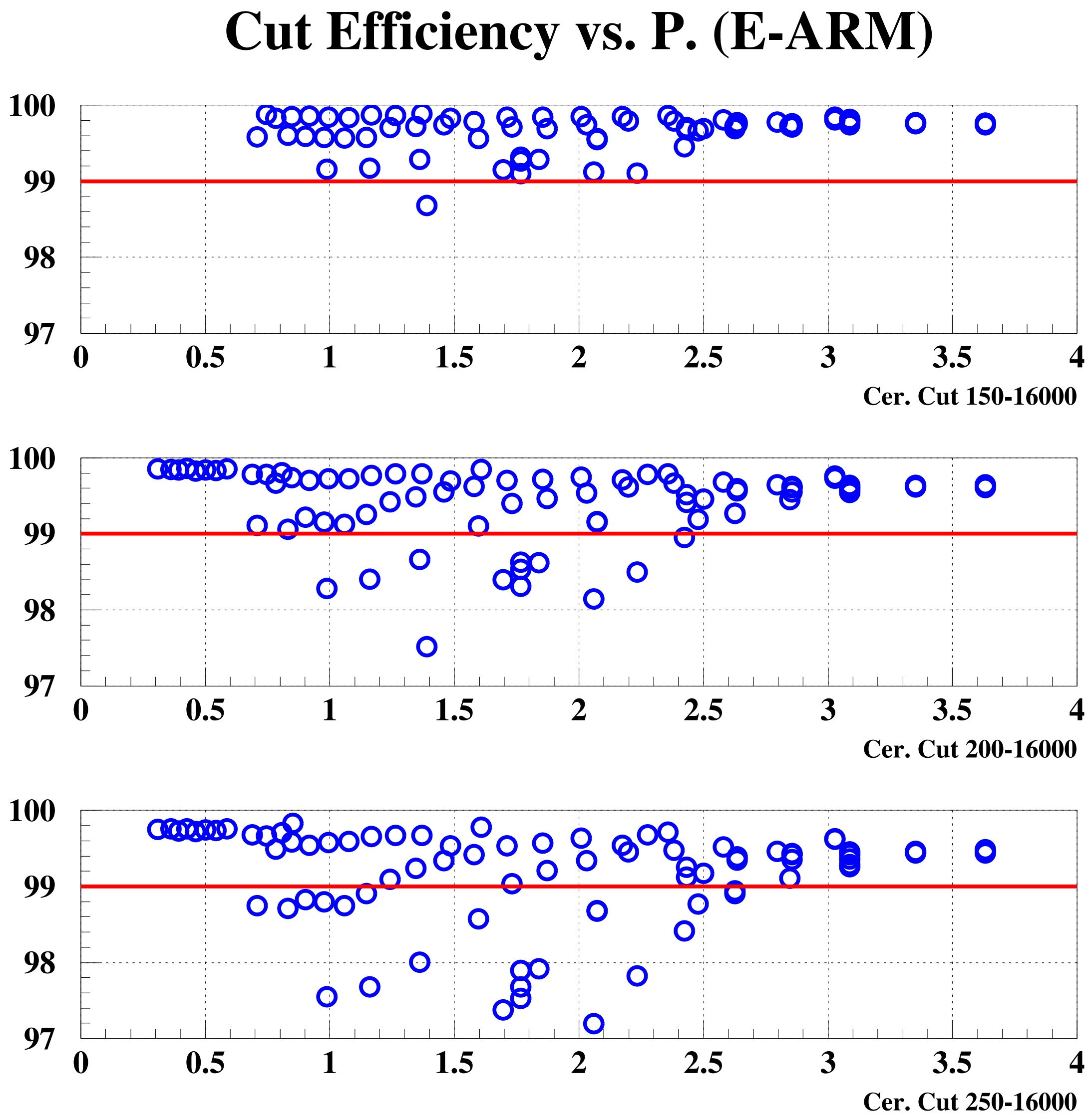

Figure 8: **Cut Efficiency as a function of momentum** (Electron Arm). Results for three different choices of the cuts are shown.

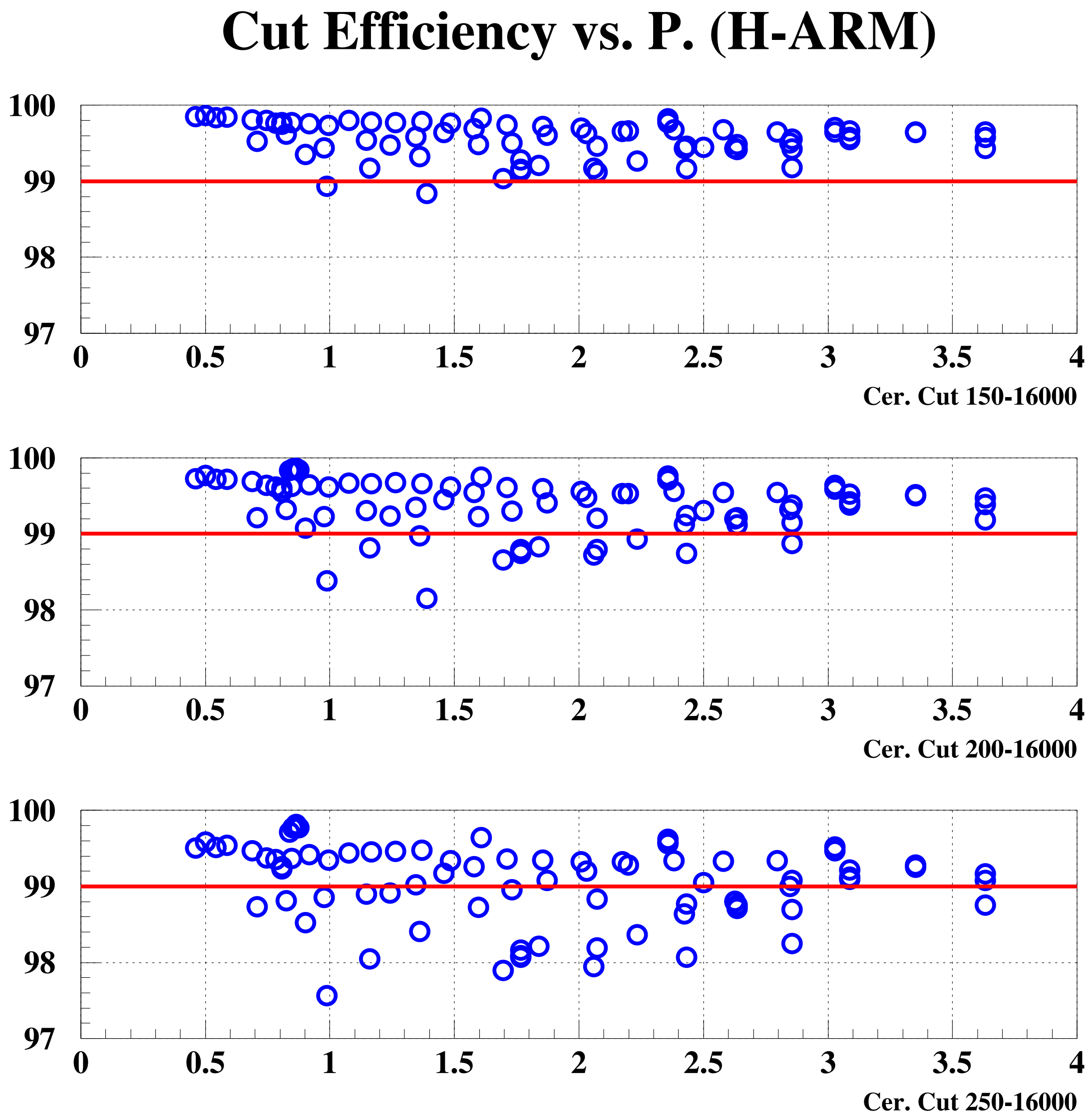

Figure 9: **Cut Efficiency as a function of momentum.** (Hadron Arm). Results for three different choices of the cuts are shown.

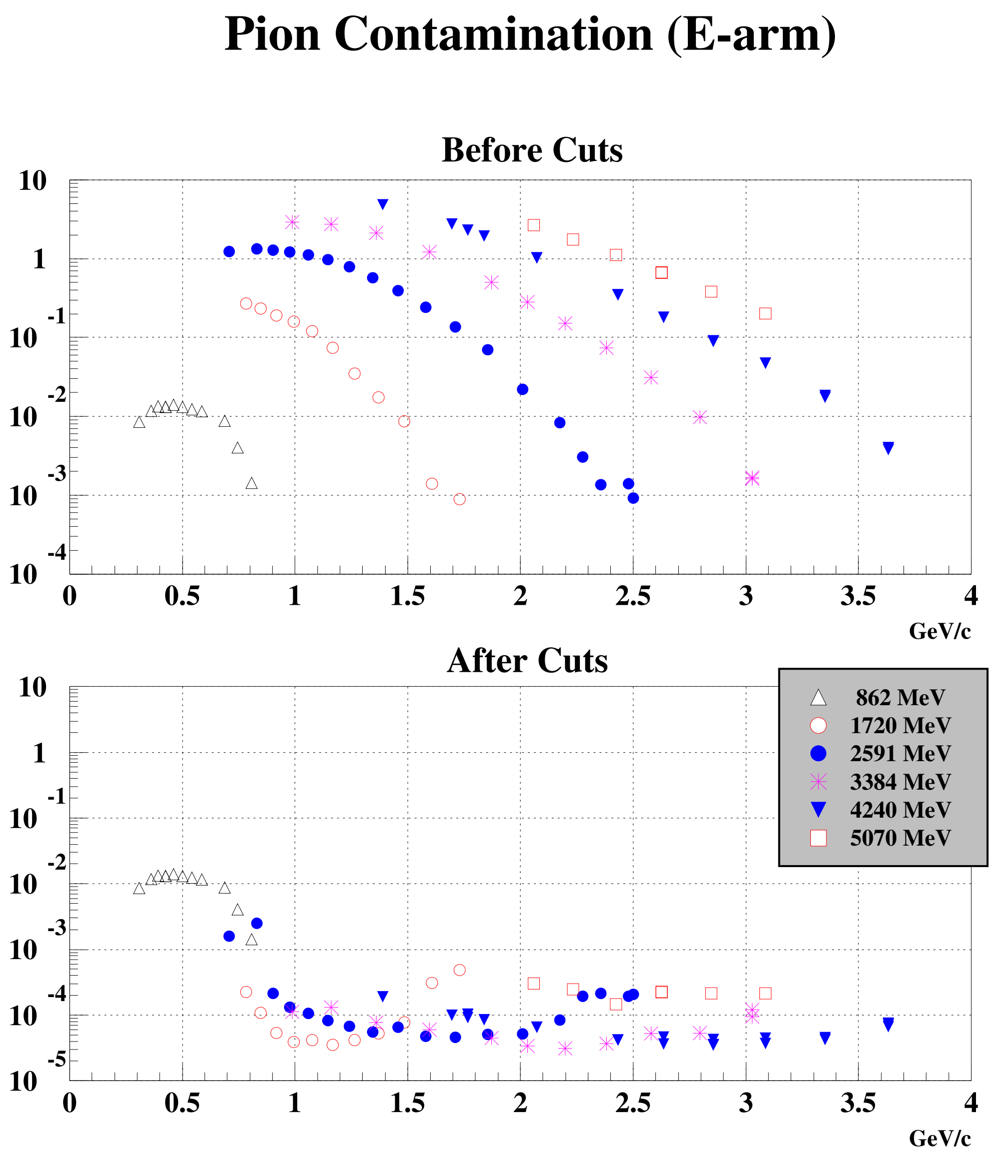

Figure 10: Effect of particle ID Cut on π/e ratio (Electron Arm).

7 Appendix: Data Tables

For reference, we include the results of the Čerenkov analysis in tabular form. The data is organized into four tables, according to whether the run is an Electron arm or Hadron arm run and whether the data was collected with a single DAQ system, or with a two DAQ system. An entry of "xxx" represents a momentum setting where ^{3}He is not the target, or that an analysis was not performed, such as Nitrogen reference cell runs, junk runs, etc. The tables are reproduced in directory ~/slifer/ceren. Column headings are explained as follows:

First : First run of a momentum setting.

Last : Last run of a momentum setting.

$\mathbf{E}_0$: Incident Energy.

$\mathbf{P}_0$: Spectrometer central momentum.

Single γ : Location of single photo-electron peak (averaged over 10 mirrors)

σ : Standard deviation of 10 mirror average.

ε_{det} : Detection Efficiency of Čerenkov.

Cut : Value of lower cut on Čerenkov spectrum. Upper cut is 16000.

ε_{cut} : Cut Efficiency.

Table 1: Single DAQ, Electron Arm							
First Last	E_0	P_0	Singleγ	σ	ε_{det}	Cut	ε_{cut}
1919 2030	3384	3.028	218.24	3.94	99.9760	150	99.8094
2031 2052	3384	2.796	213.65	2.82	99.9686	150	99.7778
2054 2068	3384	2.580	212.93	1.51	99.9611	150	99.8086
2073 2092	3384	2.382	212.83	1.40	99.9622	150	99.7953
2093 2105	3384	2.199	212.30	1.85	99.9571	150	99.7931
2106 2123	3384	2.030	211.70	1.98	99.9466	150	99.7413
2124 2137	3384	1.873	212.12	1.43	99.9279	150	99.6920
2138 2152	3384	1.596	209.17	2.36	99.9038	150	99.5604
2153 2174	3384	1.360	208.67	2.76	99.8571	150	99.2875
2175 2201	3384	1.159	208.91	3.04	99.7246	150	99.1724
2202 2218	3384	0.988	210.10	3.23	99.6499	150	99.1552
2220 2235	1720	1.607	215.32	0.70	99.9543	150	99.8978
2236 2252	1720	1.484	212.73	2.91	99.9409	150	99.8292
2253 2260	1720	1.369	212.17	2.18	99.9556	150	99.8836
2261 2268	1720	1.264	212.71	2.34	99.9452	150	99.8667
2269 2280	1720	1.167	212.27	2.27	99.9272	150	99.8715
2281 2287	1720	1.077	211.60	1.64	99.9214	150	99.8337
2291 2295	1720	0.994	211.54	2.08	99.9164	150	99.8463
2296 2302	1720	0.918	211.25	1.51	99.8959	150	99.8550
2304 2307	1720	0.847	211.17	1.44	99.8976	150	99.8470
2308 2313	1720	0.782	211.36	2.04	99.8601	150	99.8278
2314 2319	1720	1.730	211.18	4.05	99.9504	150	99.7098
2334 2372	4240	2.636	222.48	5.89	xxxxxxx	150	xxxxxxx
2373 2477	4240	3.352	215.04	4.18	99.9664	150	99.7699
2478 2543	4240	3.631	213.25	2.42	99.9746	150	99.7598
2544 2560	4240	3.086	215.08	3.96	99.9782	150	99.7416
2562 2573	4240	3.631	215.27	4.16	99.9701	150	99.7424
2574 2585	4240	3.086	215.37	4.13	99.9669	150	99.7793
2586 2597	4240	2.856	214.78	3.80	99.9751	150	99.7575
2598 2604	4240	3.631	214.50	3.83	99.9766	150	99.7622
2605 2609	4240	2.636	215.45	4.42	99.9606	150	99.7680
2610 2614	4240	2.856	xxxxxx	xxxx	99.9677	150	99.7414
2615 2626	4240	2.636	215.45	4.42	99.9670	150	99.7504
2628 2633	4240	2.433	214.90	4.40	99.9428	150	99.7065
2634 2637	4240	2.073	xxxxxx	xxxx	99.9189	150	99.5469
2639 2682	4240	1.767	210.88	3.97	99.8155	150	99.1024
2683 2688	4240	2.856	xxxxxx	xxxx	99.9573	150	99.7158
2690 2690	4240	2.636	xxxxxx	xxxx	xxxxxxx	150	xxxxxxx
2691 2693	4240	2.433	xxxxxx	xxxx	99.9475	150	99.6752
2694 2696	4240	2.073	xxxxxx	xxxx	99.9289	150	99.5597
2697 2698	4240	1.767	xxxxxx	xxxx	99.8905	150	99.3168
2699 2700	4240	1.838	xxxxxx	xxxx	99.8830	150	99.2860
2701 2702	4240	1.696	211.08	3.58	99.8350	150	99.1528
2703 2732	4240	1.389	209.62	4.06	99.7495	150	98.6803
3331 3351	5070	3.086	200.85	6.12	99.9526	150	99.8075
3352 3374	5070	2.625	197.84	4.25	99.9319	150	99.6923
3375 3386	5070	2.846	197.22	5.14	99.9391	150	99.7278
3389 3404	5070	2.233	212.00	4.31	99.8677	150	99.1055
3405 3440	5070	2.423	211.33	4.67	99.9048	150	99.4542
3441 3474	5070	2.059	209.46	4.26	99.8041	150	99.1210

Table 2: Single DAQ Hadron Arm							
First Last	E_0	P_0	Singleγ	σ	ε_{det}	Cut	ε_{cut}
1917 2030	3384	3.028	276.60	10.61	99.6975	150	99.6471
2031 2052	3384	2.796	276.91	12.05	99.5806	150	99.6465
2054 2068	3384	2.580	275.53	11.27	99.5120	150	99.6744
2073 2092	3384	2.382	276.93	13.43	99.5015	150	99.6801
2094 2105	3384	2.199	274.99	13.00	99.3829	150	99.6626
2106 2123	3384	2.030	275.27	9.590	99.2908	150	99.6265
2124 2137	3384	1.873	276.50	16.68	99.1584	150	99.6028
2138 2152	3384	1.596	270.99	11.71	98.5187	150	99.4853
2154 2174	3384	1.360	274.49	18.16	98.0078	150	99.3207
2175 2201	3384	1.159	268.95	9.050	97.1413	150	99.1717
2202 2218	3384	0.987	269.86	12.76	96.6818	150	98.9315
2220 2235	1720	1.607	272.23	1.360	99.7093	150	99.8311
2237 2252	1720	1.484	274.52	9.110	99.4848	150	99.7666
2253 2260	1720	1.369	273.50	6.460	99.5757	150	99.7837
2261 2268	1720	1.264	275.20	9.680	99.5164	150	99.7737
2269 2280	1720	1.167	273.99	8.610	99.4137	150	99.7754
2282 2287	1720	1.077	272.16	6.480	99.4428	150	99.7966
2291 2292	1720	0.994	273.36	10.68	99.3871	150	99.7366
2297 2302	1720	0.918	273.28	10.44	99.3509	150	99.7556
2304 2307	1720	0.847	273.19	8.080	99.2850	150	99.7730
2308 2313	1720	0.782	273.45	7.790	99.2049	150	99.7636
2314 2314	1720	1.163	xxxxx	xxxxxx	xxxxxxx	150	xxxxxxx
2315 2319	1720	1.730	275.14	10.85	99.8478	150	99.5061
2334 2372	4240	2.636	287.69	14.90	xxxxxxx	150	xxxxxxx
2375 2421	4240	3.086	272.52	7.510	99.5085	150	99.6443
2422 2481	4240	2.856	277.12	8.050	99.4606	150	99.6429
2482 2555	4240	2.636	278.07	7.060	99.3202	150	99.6478
2556 2597	4240	2.433	274.75	9.900	99.2553	150	99.5784
2599 2637	4240	2.073	276.62	7.490	98.6919	150	99.4311
2640 2698	4240	1.767	272.41	10.17	97.5033	150	99.1387
2699 2700	4240	1.838	xxxxx	xxxxxx	97.9110	150	99.2111
2701 2702	4240	1.696	272.78	11.33	97.4297	150	99.0322
2703 2732	4240	1.389	273.23	11.02	95.8300	150	98.8392
3331 3351	5070	3.086	280.93	11.85	99.3215	150	99.5451
3359 3374	5070	2.625	279.45	14.82	98.9771	150	99.4297
3379 3386	5070	2.846	275.21	11.78	99.1618	150	99.5066
3389 3404	5070	2.233	270.53	11.29	98.1064	150	99.2655
3405 3440	5070	2.423	271.85	15.43	98.7234	150	99.4320
3441 3474	5070	2.059	271.45	15.16	97.5349	150	99.1717
3478 3479	5070	2.625	xxxxx	xxxxxx	xxxxxxx	150	xxxxxxx
3480 3480	5070	2.846	xxxxx	xxxxxx	xxxxxxx	150	xxxxxxx

Table 3: Two DAQ, Hadron Arm							
First Last	E_0	P_0	Singleγ	σ	ε_{det}	Cut	ε_{cut}
2747 2751	0862	0.851	272.12	19.44	99.8049	150	99.9132
2752 2762	0862	0.808	268.48	20.16	99.2319	150	99.7474
2763 2775	0862	0.746	268.68	17.35	99.4032	150	99.7975
2776 2789	0862	0.689	270.26	17.09	99.5043	150	99.8049
2790 2797	0862	0.587	271.72	14.18	99.4821	150	99.8425
2798 2803	0862	0.542	270.84	12.55	99.5063	150	99.8352
2804 2807	0862	0.500	271.19	14.27	99.4765	150	99.8643
2808 2814	0862	0.461	270.59	13.13	99.4576	150	99.8465
2815 2815	0862	0.434	272.75	15.23	xxxxxxx	150	xxxxxxx
2818 2835	0862	0.808	262.53	20.39	99.2921	150	99.7732
2836 2841	0862	0.864	xxxxxx	xxxxx	xxxxxxx	150	xxxxxxx
2842 2842	0862	0.877	xxxxxx	xxxxx	xxxxxxx	150	xxxxxxx
2843 2844	0862	0.876	252.41	21.00	99.8387	150	99.8919
2845 2851	0862	0.864	251.07	23.62	99.8540	150	99.9149
2852 2854	0862	0.838	246.11	25.49	99.8095	150	99.9022
2855 2865	0862	0.864	250.24	26.36	99.8634	150	99.9260
2866 2869	0862	0.826	256.24	26.44	98.6198	150	99.6214
2871 2885	0862	0.862	xxxxxx	xxxxx	xxxxxxx	150	xxxxxxx
2886 2888	0862	0.897	xxxxxx	xxxxx	xxxxxxx	150	xxxxxxx
2889 2907	0862	0.880	xxxxxx	xxxxx	xxxxxxx	150	xxxxxxx
2908 2916	0862	0.845	xxxxxx	xxxxx	xxxxxxx	150	xxxxxxx
2917 2925	0862	0.828	xxxxxx	xxxxx	xxxxxxx	150	xxxxxxx
2926 2930	0862	0.863	xxxxxx	xxxxx	xxxxxxx	150	xxxxxxx
2943 2947	2591	2.501	278.52	13.01	99.7670	150	99.4461
2949 2998	2591	2.357	275.18	13.66	99.6770	150	99.7703
2999 3021	2591	2.175	272.19	16.29	99.5880	150	99.6518
3023 3038	2591	2.008	270.53	13.14	99.5018	150	99.6975
3040 3050	2591	1.854	270.82	15.14	99.4807	150	99.7166
3051 3063	2591	1.711	268.99	11.37	99.4525	150	99.7433
3064 3072	2591	1.579	270.77	15.37	99.3890	150	99.6905
3073 3085	2591	1.458	269.31	12.97	99.2441	150	99.6380
3086 3104	2591	1.346	272.37	14.42	99.0632	150	99.5817
3105 3133	2591	1.242	271.43	9.030	98.8709	150	99.4727
3134 3146	2591	1.147	265.14	12.69	98.6448	150	99.5429
3148 3164	2591	0.902	266.46	14.67	98.3624	150	99.3556
3165 3176	2591	0.709	265.46	12.78	98.2902	150	99.5249
3177 3190	2591	0.977	269.46	16.44	98.3744	150	99.4351
3191 3205	2591	1.059	265.78	11.04	xxxxxxx	150	xxxxxxx
3206 3213	2591	0.832	267.75	14.25	xxxxxxx	150	xxxxxxx
3214 3215	2591	0.848	266.95	13.05	xxxxxxx	150	xxxxxxx
3216 3216	2591	0.816	xxxxxx	xxxxx	xxxxxxx	150	xxxxxxx
3227 3258	2591	2.530	262.77	17.59	xxxxxxx	150	xxxxxxx
3259 3269	2591	2.580	261.78	23.22	xxxxxxx	150	xxxxxxx
3272 3298	2591	2.275	261.61	16.89	xxxxxxx	150	xxxxxxx
3306 3324	5070	3.086	xxxxxx	xxxxx	xxxxxxx	150	xxxxxxx

Table 4: Two DAQ, Electron Arm							
First Last	E_0	P_0	Singleγ	σ	ε_{det}	Cut	ε_{cut}
20121 20122	0862	0.851	214.45	4.73	99.9055	150	99.9325
20123 20133	0862	0.808	210.57	4.50	99.9015	150	99.8912
20134 20143	0862	0.746	204.33	8.64	99.8976	150	99.8800
20144 20154	0862	0.689	204.42	7.59	99.8993	150	99.9011
20155 20162	0862	0.587	205.86	6.15	99.8728	150	99.9203
20163 20168	0862	0.542	206.10	5.98	99.8665	150	99.9264
20169 20172	0862	0.500	205.93	5.89	99.8598	150	99.9284
20174 20180	0862	0.461	206.52	5.57	99.8559	150	99.9241
20181 20198	0862	0.426	206.42	6.30	99.8355	150	99.9191
20199 20209	0862	0.393	203.78	6.14	99.8193	150	99.9180
20210 20218	0862	0.363	203.18	5.94	99.8142	150	99.9243
20219 20229	0862	0.309	204.93	5.26	99.7850	150	99.9290
20230 20277	0862	0.828	xxxxxx	xxxx	xxxxxxx	150	xxxxxxx
20289 20293	2591	2.501	217.85	6.08	99.9602	150	99.6918
20294 20343	2591	2.357	209.83	4.18	99.9636	150	99.8627
20344 20361	2591	2.175	209.77	4.45	99.9538	150	99.8482
20364 20379	2591	2.008	209.61	3.04	99.9591	150	99.8517
20380 20391	2591	1.854	209.29	3.19	99.9513	150	99.8399
20392 20404	2591	1.711	209.13	2.54	99.9477	150	99.8392
20405 20413	2591	1.579	208.75	2.57	99.9350	150	99.7835
20414 20426	2591	1.458	209.28	2.93	99.9259	150	99.7426
20428 20444	2591	1.346	211.03	2.56	99.9244	150	99.7218
20445 20462	2591	1.242	212.17	3.31	99.8906	150	99.7034
20463 20477	2591	1.147	209.05	2.44	99.8500	150	99.5781
20479 20498	2591	0.902	207.90	3.52	99.7430	150	99.5907
20499 20510	2591	0.709	207.78	2.67	99.6371	150	99.5835
20511 20526	2591	0.977	207.45	3.42	99.7724	150	99.5723
20527 20539	2591	1.059	208.67	2.97	99.8253	150	99.5686
20540 20547	2591	0.832	193.28	4.38	99.6204	150	99.6023
20548 20548	2591	0.848	xxxxxx	xxxx	xxxxxxx	150	xxxxxxx
20549 20549	2591	0.816	xxxxxx	xxxx	xxxxxxx	150	xxxxxxx
20550 20556	2591	2.479	193.95	4.01	99.9621	150	99.6619
20557 20579	2591	2.273	xxxxxx	xxxx	xxxxxxx	150	xxxxxxx
20581 20606	2591	2.275	195.53	4.28	99.9625	150	99.8997
20608 20621	5070	3.086	xxxxxx	xxxx	99.9579	150	99.7869